Journal of Food and Drug Analysis

Volume 31 | Issue 2 Article 12

Urolithin A exhibits a neuroprotective effect against Alzheimer's disease by inhibiting DYRK1A activity

Recommended Citation

Tu, Huang-Ju; Su, Chih-Jou; Peng, Chao-Shiang; Lin, Tony Eight; Huang Fu, Wei-Chun; Hsu, Kai-Cheng; Hwang, Tsong-Long; and Pan, Shiow-Lin (2023) "Urolithin A exhibits a neuroprotective effect against Alzheimer's disease by inhibiting DYRK1A activity," *Journal of Food and Drug Analysis*: Vol. 31 : Iss. 2 , Article 12.
Available at: https://doi.org/10.38212/2224-6614.3462

ORIGINAL ARTICLE

Urolithin A exhibits a neuroprotective effect against Alzheimer's disease by inhibiting DYRK1A activity

Huang-Ju Tu [a,1], Chih-Jou Su [b,1], Chao-Shiang Peng [b], Tony Eight Lin [a,c], Wei-Chun HuangFu [a,b,c,d,e], Kai-Cheng Hsu [a,b,c,d,e], Tsong-Long Hwang [g,h,i,j,**], Shiow-Lin Pan [a,b,c,d,e,f,*]

[a] Graduate Institute of Cancer Biology and Drug Discovery, College of Medical Science and Technology, Taipei Medical University, No.250, Wu-Xing Street, Xinyi Dist., Taipei 110, Taiwan
[b] Ph.D. Program for Cancer Molecular Biology and Drug Discovery, College of Medical Science and Technology, Taipei Medical University, No.250, Wu-Xing Street, Xinyi Dist., Taipei 110, Taiwan
[c] Master Program in Graduate Institute of Cancer Biology and Drug Discovery, College of Medical Science and Technology, Taipei Medical University, No.250, Wu-Xing Street, Xinyi Dist., Taipei 110, Taiwan
[d] Ph.D. Program in Drug Discovery and Development Industry, College of Pharmacy, Taipei Medical University, No.250, Wu-Xing Street, Xinyi Dist., Taipei 110, Taiwan
[e] TMU Research Center of Cancer Translational Medicine, Taipei Medical University, No.250, Wu-Xing Street, Xinyi Dist., Taipei 110, Taiwan
[f] TMU Research Center of Drug Discovery, Taipei Medical University, No.250, Wu-Xing Street, Xinyi Dist., Taipei 110, Taiwan
[g] Graduate Institute of Natural Products, College of Medicine, Chang Gung University, No.259, Wenhua 1st Rd., Guishan Dist., Taoyuan City 333, Taiwan
[h] Research Center for Chinese Herbal Medicine, Graduate Institute of Healthy Industry Technology, College of Human Ecology, Chang Gung University of Science and Technology, No.261, Wenhua 1st Rd., Taoyuan City 33303, Taiwan
[i] Department of Anesthesiology, Chang Gung Memorial Hospital, No.5, Fuxing St., Guishan Dist., Taoyuan City 333, Taiwan
[j] Department of Chemical Engineering, Ming Chi University of Technology, No.84 Gungjuan Rd., New Taipei City 243303, Taiwan

Abstract

Alzheimer's disease (AD) is a devastating neurodegenerative disease with more than 50 million people suffer from it. Unfortunately, none of the currently available drugs is able to improve cognitive impairment in AD patients. Urolithin A (UA) is a metabolite obtained from ellagic acid and ellagitannin through the intestinal flora, and it has antioxidant and anti-inflammatory properties. Previous reports found that UA had neuroprotective effects in an AD animal model, but the detailed mechanism still needs to be elucidated. In this study, we performed kinase-profiling to show that dual-specific tyrosine phosphorylation-regulated kinase 1A (DYRK1A) is the main target of UA. Studies showed that the level of DYRK1A in AD patients' brains was higher than that of healthy people, and it was closely related to the occurrence and progression of AD. Our results revealed that UA significantly reduced the activity of DYRK1A, which led to de-phosphorylation of tau and further stabilized microtubule polymerization. UA also provided neuroprotective effects by inhibiting the production of inflammatory cytokines caused by Aβ. We further showed that UA significantly improved memory impairment in an AD-like mouse model. In summary, our results indicate that UA is a DYRK1A inhibitor that may provide therapeutic advantages for AD patients.

Keywords: Alzheimer's disease, DYRK1A, Tau, Urolithin A

List of abbreviations: Aβ, Amyloid β; AD, Alzheimer's Disease; APP, amyloid precursor protein; DS, Down syndrome; DYRK1A, Dual-specific tyrosine phosphorylation-regulated kinase 1A; i.c.v, intracerebroventricular; MTT, 3-[4,5-dimethylthiazol-2-yl]-2,5 diphenyl tetrazolium bromide; NFTs, Neurofibrillary tangles; NMDA, N-methyl-D-aspartate; OA, Okadaic acid; UA, Urolithin A.

Received 6 January 2023; accepted 10 April 2023.
Available online 15 June 2023

* Corresponding author. Graduate Institute of Cancer Biology and Drug Discovery, College of Medical Science and Technology, Taipei Medical University, No.250, Wu-Xing Street, Xinyi Dist., Taipei, 110, Taiwan.
** Corresponding author. Graduate Institute of Natural Products, College of Medicine, Chang Gung University, No.259, Wenhua 1st Rd., Guishan Dist., Taoyuan City, 333, Taiwan.
E-mail addresses: htl@mail.cgu.edu.tw (T.-L. Hwang), slpan@tmu.edu.tw (S.-L. Pan).
[1] These authors contributed equally to this work and share first authorship.

https://doi.org/10.38212/2224-6614.3462

1. Introduction

Alzheimer's disease (AD) is the most common cause of dementia, accounting for 60%−70% of dementia cases. Drugs used for AD treatment are mainly divided into two categories, acetylcholinesterase inhibitors and N-methyl-D-aspartate (NMDA) receptor antagonists, both of which can help temporarily improve certain symptoms. However, none of these drugs can reverse or even slow down the development of AD. Therefore, there is an urgent need to develop drugs for AD.

The main neuropathological features of AD include extracellular amyloid β (Aβ) which forms senile plaques and the accumulation of neurofibrillary tangles (NFTs) composed of hyperphosphorylated tau protein in cells. Since Aβ and NFTs are two major risk factors in the pathogenesis of AD, most drugs were designed to target Aβ and tau [1]. Despite positive data from early-stage clinical trials, only a few drugs showed promising clinical benefits in phase III clinical trials. One of the reasons causing drugs to fail in humans is the timing of treatment. Neuronal damage caused by the accumulation of Aβ and NFT can occur 10−30 years before the onset of AD [2], so any treatment may be too late when a patient already has neuronal loss. Another question is the limitation of early detection, in that it is hard to produce a routine test using current diagnostic tools such as computed tomography (CT) or magnetic resonance imaging (MRI) before patients showed early signs of AD, and the sensitivity of these examinations is also a big issue [3]. Therefore, our strategy was to prevent the development of AD by using a natural remedy as daily supplements since they are relative safe and easy to obtain.

Natural plants have garnered attention due to their ability to delay the onset and alleviate the symptoms of AD with relatively few side effects compared to conventional drugs [4]. Recently, an article by Yuan et al. pointed out that urolithins, which are gut microbic metabolites of ellagitannins, play a crucial role in neuroprotection [5]. Among the urolithin derivatives, urolithin A (UA) is the main metabolite in human plasma [6] and urine, and has its impacts on aging, muscle dysfunctions, cardiovascular diseases, brain diseases and cancer [7]. A previous study showed that UA may be beneficial in an AD's animal model [8], as daily treatment with UA ameliorated learning and memory deficits in APP/PS1 transgenic mice. Another study showed that daily injections of UA reduced APP expression, tau phosphorylation, and cognitive impairment in a streptozotocin (STZ)-induced diabetic mouse model [9]. However, how could UA provide these benefits is unclear. The goal of this study is to uncover the potential target of UA by using structure-based virtual screening approach and further explore the underlying mechanism of how UA provide neuroprotective effect for AD.

2. Materials and methods

2.1. Materials and cell lines

The HEK-293 human embryonic kidney cell line (Bioresource Collection and Research Center (BCRC), 60019) were maintained in modified Eagle's medium (MEM, Life Technologies, Inc.) containing nonessential amino acids and supplemented with 10% (v/v) fetal bovine serum (FBS). The COS-7 green monkey kidney cell line (BCRC, CVCL_0224) was maintained in Dulbecco's modified minimal essential medium (DMEM) (Life Technologies, Inc.) supplemented with 10% (v/v) FBS. The BV-2 mouse microglial cell line was a generous gift from Dr. Chen, Yun-Ru (Laboratory for Protein misfolding and neurodegenerative diseases, Genomics Research Center, Academia Sinica). BV-2 cell was maintained in DMEM supplemented with 10% (v/v) FBS. All cells were incubated in 37 °C incubators containing 5% CO_2.

Urolithin A was purchased from Combi-Blocks (San Diego, CA, USA). INDY and okadaic acid were obtained from Abcam (Cambridge, UK). Primary antibodies DYRK1A (#2771), Tau441 (#46687), Thr181-Tau (#12885) and Thr217-Tau (#35834) were purchased from Cell Signaling Technology (MA, USA). Ser199/202-Tau (44-768G) and Thr212-Tau (44-740G) were obtained from Thermo Fisher Scientific (MA, USA).

2.2. Molecular docking

The DYRK1A (PDB ID: 5A4E) protein structure was obtained from the Protein Data Bank [10]. The Schrodinger Maestro computational software was used to prepare the protein structure and the compound using the Protein Preparation Wizard and LigPrep modules, respectively. The receptor grid was generated using default settings with the co-ligand as the centroid object. Docking was performed using the Glide module [11] using default settings. The 3D image of the docked compounds was generated using PyMoL.

2.3. Protein kinase activity assay

To identify the potential target of selected compound, protein kinase activity was conducted by Z′-

LYTE™ kinase assay provided by Thermos Fisher Scientific (www.thermofisher.com/selectscreen). Briefly, the selected compound, ATP, selected kinases and a synthetic FRET (Fluorescence Resonance Energy Transfer)-peptide were incubated for 1 h. The kinase inhibition activity was determined by the emission ratio which calculates the donor emission to acceptor emission after excitation of the donor fluorophore at 400 nm.

2.4. Cell viability test

The cell viability was measured by MTT assay. In brief, cells at a density of 5×10^3 cells per well were seeded in 96-well plates. After 24 h, cells were incubated with indicated concentrations of UA for 48 h, DMSO was used as solvent control. Then cells were incubated with MTT (0.5 mg/mL in PBS) for 2 h at 37 °C. Finally, the culture mediums were substituted with 100 μL DMSO and the absorption was measured at 550 nm by an ELISA reader (Molecular Devices, Sunnyvale, CA, USA). Results are performed as the percentage of MTT reaction, assuming that the absorbance of the control cells was 100%.

2.5. Plasmid construction

The pEGFP-C1 vector and pET-28a (+) vector containing human Tau cDNA encoding 441 amino acids were kindly provided by Dr. Ko, Chiung-Yuan from Ph.D. Program for Neural Regenerative Medicine, College of Medical Science and Technology, Taipei Medical University (Taiwan). The mammalian expression plasmid for the DYRK1A was constructed into a pDsRed-Monomer-Hyg-C1 vector (Clontech). The sequences of primers used to construct the plasmid were pDsRed-Monomer-Hyg-C1: upstream primer Xho1 5′-CCCCCCCTCGAGCCATGCATA CAGGAGGAGAGACT- 3′ and downstream primer Kpn1 5′-CCCCCCGGTACCCGAGCTAGCTACAG GACTCTG-3'. Pfu DNA Polymerase (M774A, Promega) was used according to the manufacturer's instructions for polymerase chain reaction (PCR). Subsequently, the purified PCR products were digested with restriction enzyme pairs (FastDigest Restriction Enzymes, Thermo Scientific) and ligated with T4 DNA ligase (NEB) to pDsRed-Monomer-Hyg-C1.

2.6. Sample preparation and western blot

Cells were seeded in 6-well plates at a density of 3×10^5 cells per well and incubated overnight before the experiment. The cells were co-transfected with pDsRed-DYRK1A and EGFP-Tau plasmid by Opti-MEM and Lipofectamine® 2000 (Lifescience) system for 24 h. Then cells were treated with indicated concentration of UA or INDY for 24 h. The cells were lysed in RIPA buffer with protease inhibitor cocktail. Pierce™ BCA Protein Assay Kit (23227, ThermoFisher) was used to determine the total amount of protein. Each sample was adjusted to the same protein concentration and then mixed with 5X protein sample buffer and heated at 97 °C for 5 min. The equal amount of total proteins were electrophoresed through sodium dodecyl sulfate-polyacrylamide gel (SDS-PAGE) and transferred to PVDF membranes. After incubation with 2% BSA in TBST, the membrane was incubated with indicated primary antibodies at 4 °C overnight. Then membranes were washed with TBST for three times every 15 min. HRP-conjugated secondary antibodies were diluted in 2% BSA in TBST and incubated with the membranes on a shaker for 1 h at room temperature, followed by the membranes washed with TBST for three times every 15 min. Bound antibodies were measured using the ECL system (GE Healthcare Amersham), and the membranes were placed on a photographic film.

2.7. Tubulin assembly assay

Tubulin assembly assay was conducted in a cell-free system and performed according to the protocol of the tubulin polymerization assay kit (BK006P, Cytoskeleton, Denver, CO, USA) from the manufacturer with some modifications. The p-tau were made by mixing 11 μg human recombinant Tau441 protein with 0.75 μg DYRK1A for 150 min at 30 °C in kinase buffer (20 mM MOPS pH 7.0, 10 mM $MgCl_2$, 1 mM DTT, 20 μM sodium orthovanadate, and 0.3 mM ATP). In brief, 96-well plate was preheated in a spectrophotometer at 37 °C before the experiment. Tubulin polymerization (TP) buffer was prepared on ice by mixing 750 μL general tubulin buffer (80 mM PIPES pH 6.9, 2 mM $MgCl_2$, 0.5 mM EGTA), 250 μL tubulin glycerol buffer (15% glycerol in general tubulin buffer), and 10 μL 100 mM GTP Stock. Subsequently, 10 μL of 0.37 μg/μL human recombinant tau protein or previously prepared p-tau were added to the 96-well plate and place in a 37 °C spectrophotometer for 2 min. Tubulin was thawed at room temperature and diluted with TP buffer to 1 μg/μL on ice. 100 μL of tubulin solution was added to the 96-well plate containing tau or p-Tau. After mixing, the 340 nm absorbance was measured continuously in a spectrophotometer at 37 °C every 1 min for a total of 60 min.

2.8. Oligomeric Aβ preparation

Aβ peptide (AS-24224, AnaSpec, CA, USA) was dissolved in DMSO and further diluted to 200 μM with cold PBS buffer. The diluted Aβ was equally mixed with ice-cold serum-free F12 medium. To prevent aggregation, the Aβ solution was further sonicated (60 Hz, 25 W) for 20 s on/off for 2 times and then centrifuged for 15 min at 14000 g to remove insoluble clumps. Finally, the soluble monomeric Aβ were incubated at 4 °C for 24 h to yield oligomeric Aβ.

2.9. Quantitative real-time PCR for mRNA analysis

Cells were cultured onto 6 wells plates and treated with indicated compounds. Total RNA was extracted from cells with TRIzol kit (Thermo Fisher Scientific, MA, USA). Single-strand cDNA was synthesized using One-Step RT-qPCR Kit from ZYMO Research (Irvine, CA, USA). After that cDNA was amplified with specific primers for IL-6, TNF-α and 18S genes. The results were carried out in triplicate on a StepOnePlus (Applied Biosystems, CA) sequence detection system. Gene expression levels were calculated by using formula $2^{-\Delta\Delta CT}$. Specific PCR primers used were as follows:

mouse 18S:
forward, GCAATTATTCCCCATGAACG;
reverse, GGCCTCACTAAACCATCCAA
mouse IL-6:
forward, GAGGATACCACTCCCAACAGACC;
reverse, AAGTGCATCATCGTTGTTCATACA
mouse TNF-α:
forward, GGTGCCTATGTCTCAGCCTCTT;
reverse, GCCATAGAACTGATGAGAGGGAG.

2.10. Animals

The experimental timeline is described in Fig. 6A. 8-week male C57BL/6J mice were purchased from BioLASCO Taiwan Co., Ltd. Animals were housed under standard conditions of light and dark cycle with free access to food and water ad libitum. All procedures were performed in accordance with the NIH guidelines on laboratory animal welfare, and the study was approved by the Taipei Medical University Animal Care and Use Committee (LAC-2020-0472).

2.11. Intracerebroventricular injection

After habituation, mice were treated with vehicle (saline) or UA (100 mg/kg, i.p., qd) for three days and followed by intracerebroventricular (i.c.v) injection of okadaic acid (OA, 100 ng/μL, 10 μL). During surgical procedures, the animals were anesthetized with zoletil/xylazine and restrained in a stereotaxic apparatus (Stoelting, Wood Dale, IL, USA). OA was dissolved in artificial CSF (147 mM NaCl; 2.9 mM KCl; 1.6 mM $MgCl_2$; 1.7 mM $CaCl_2$ and 2.2 mM dextrose) and injected into the left lateral cerebral ventricle at the following coordinates: 0 mM posterior; 2.0 mM lateral; −2.5 mM ventral to bregma through Hamilton microliter syringe. The scalp was securely sutured and mice were returned to their home cages to recover.

2.12. Morris water maze

Twelve days after i.c.v surgery, Morris water maze was used to evaluate the spatial memory of mice. A circular pool (100 cm in diameter, 50 cm high, divided into four quadrants: I, II, III, and IV) with 30 cm deep water at 25 ± 1 °C was used for the Morris water maze test. The III quadrant contained a security platform that was 1 cm below the water level. Various geometric images are placed on the wall so that the animals can use these visual cues. The test included training phase and testing phase. In training phase, mice were trained twice a day with a 2 h inter-trial interval for 4 constitutive days. The mice were allowed to swim for 60 s to find the platform. If the mice failed to find the platform in 60 s, they were placed on the platform for 20 s. On the fifth day (testing phase), platform was removed and mice were allowed to swim for 60 s. The escape latency (time spent in the III quadrant) and swimming distance were recorded. The movement of mice was tracked with a video camera and recorded by EthoVision XT (Noldus, Wageningen, the Netherlands).

2.13. Data analysis and statistics

Each result represents the mean ± SEM of at least three independent experiments. One-way ANOVA was used to analyze the data by using GraphPad Prism software. Parameters with a p-value <0.05 were considered statistically significant.

3. Results

3.1. UA directly binds to a dual-specific tyrosine phosphorylation-regulated kinase-1A (DYRK1A) -binding site and further reduces its kinase activity

UA was reported to provide protective effects in neurodegenerative diseases; however, the mechanism of UA is unclear. To identify the target of UA, UA was tested for inhibitory activity against 40 kinases which covered seven major groups of human protein kinases

(Fig. 1A). Results revealed that 3 μM UA demonstrated an inhibitory effect (inhibition of >50%) against five kinases, including DYRK1A, MINK1, MKNK1, STK3 and VRK2. Among these five kinases, UA had the greatest inhibitory activity (75%) against DYRK1A (Fig. 1B).

A biochemical kinase assay from ThermoFisher was used to determine the inhibitory activity of UA against DYRK1A at different concentrations, and it showed that UA dose-dependently inhibited the activity of DYRK1A, with a half maximal inhibitory concentration (IC_{50}) of 909 nM (Fig. 2A). We further tested the inhibitory activity of UA with various ATP concentrations. It showed that with an ATP concentration of 10 μM UA had a 97% inhibitory effect against DYRK1A. Increasing the ATP concentration led to reductions in the DYRK1A inhibitory effect. These results indicated that UA might be an ATP-competitive inhibitor to DYRK1A. To determine the molecular interactions of UA, we performed a molecular docking analysis. The docking results showed that the compound favorably occupied the DYRK1A binding site (Fig. 2C). Two hydrogen bonds were observed between UA and DYRK1A-binding site residues. UA contains a hydroxyl moiety at the C2 position that functions as a hydrogen donor to the carbonyl backbone of residue E239. A hydrogen bond with the hinge region is important for small-molecule kinase inhibitors. An additional hydrogen bond was observed between the carbonyl at the C6 position of UA and residue D307. The three-ring structure of UA was also sandwiched by hydrophobic interactions with residues in the DYRK1A-binding site. These include interactions with hydrophobic residues, such as V173, A186, L241, L294 and V306. Residue K188 further contributed to a hydrophobic interaction through its long carbon tail. Together, these results suggested that UA can effectively bind to the DYRK1A-binding site and further interfere with the activity of DYRK1A.

3.2. UA effectively inhibits DYRK1A-induced tau phosphorylation

Since tau is a direct downstream target of DYRK1A, it is a great tool to validate the effect of UA on DYRK1A activity by testing the phosphorylation status of tau. We established an *in vitro* model to overexpress DYRK1A and tau in HEK293 and COS-7 cell lines. Increases in phosphorylation of tau protein at Thr181, Thr212, Thr217, and Ser199/202 were observed (Fig. 3A and B). Treatment with UA reduced the phosphorylation of T212, T181, T217, and S199/202 in a concentration-dependent manners. This indicates that UA has the ability to reduce

A

Kinase	% Inhibition (3 μM)	Kinase	% Inhibition (3 μM)
AKT1	7	MAP3K5	-47
AURKA	31	MAP3K9	13
BRAF	9	MAPK3	4
BTK	10	MARK3	17
CAMK2B	18	MINK1	59
CDK2	50	MKNK1	53
DAPK1	39	NEK1	12
DCAMKL1	-3	NTRK1	22
DYRK1A	75	PAK2	3
EPHA3	3	PIM1	32
ERBB4	7	PRKACA	5
FGFR1	5	PRKCA	17
FLT3	39	ROCK1	28
HIPK1	34	RSK2	18
ICK	7	SRC	16
IKBKB	7	STK3	59
IRAK4	2	TGFBR1	21
LCK	18	ULK1	7
LIMK2	7	VRK2	56
MAP2K1	13	WEE1	13

B

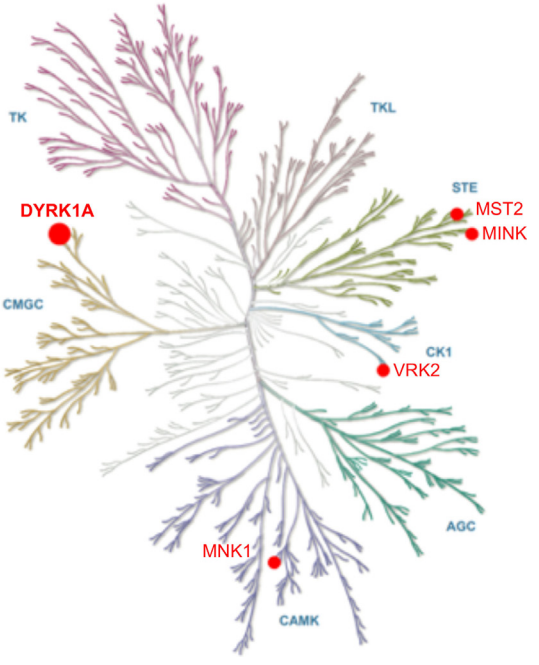

Fig. 1. ***Selectivity profile of urolithin A (UA).*** *(A) UA at 3 μM was tested against a panel of 40 kinases across the human KinMap. (B) Of all kinases, DYRK1A, MINK1, MKNK1, STK3 and VRK2 were inhibited by UA with an inhibition percentage of >50%. UA was the most selective against DYRK1A.*

A

Name	Concentration (nM)	% Inhibition
Urolithin A	10000	93
	3000	75
	1000	54
	300	26
	100	9

B

Name	ATP	% Inhibition (3 μM)
Urolithin A	1000	41
	100	75
	10	97

C

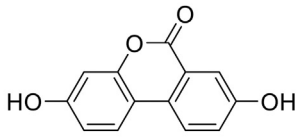

Urolithin A

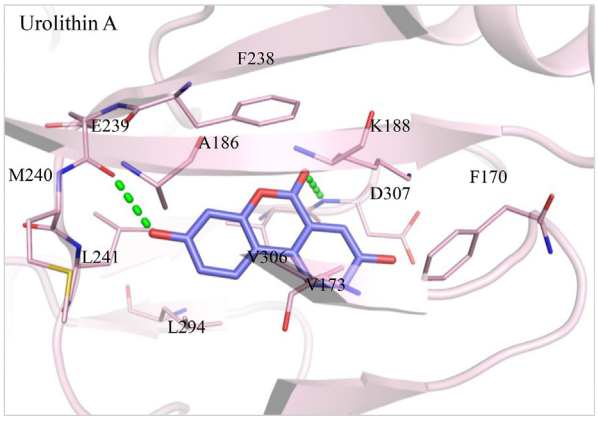

Fig. 2. ***Docking pose of urolithin A (UA) in the DYRK1A-binding site.*** *(A) The inhibitory effect of UA against DYRK1A at the indicated concentration. (B) The inhibitory effect of UA (3 μM) against DYRK1A at different concentrations of ATP. (C) UA and DYRK1A are represented by purple and pink, respectively. Hydrogen bonds are represented as green dash lines. Binding site residues are listed as shown.*

DYRK1A activity and further decrease DYRK1A-induced tau phosphorylation. Quantitative ratios of phosphorylated tau at different sites are shown in Fig. 3C–F. INDY is a non-specific DYRK family inhibitor and was used as a positive control. We further confirmed that UA had no cytotoxicity effects in HEK293 or COS-7 cells (Fig. 3G and H).

3.3. UA recovered microtubule stabilization by reducing tau phosphorylation

The tau protein plays a pivotal role in maintaining axon stability in normal physiological conditions [12]. AD patients often exhibits tau hyperphosphorylation, which disrupts the preassembled microtubules and reduces axonal transportation [13]. We established a cell-free tubulin-assembling system to test the effect of UA. It showed that the recombinant tau protein alone steadily increased turbidity by driving tubulin assembly. When recombinant DYRK1A and the tau protein were simultaneously added to the tubulin solution, it caused the depolymerization of tubulin and decreased the turbidity. Inhibition of DYRK1A by adding UA dose-dependently stabilized tubulin and increased the turbidity (Fig. 4A). We further tested the phosphorylated status of the tau protein. Results showed that UA indeed inhibited the phosphorylation of tau at pT181, pT212, and pT199/202 in a cell-free system (Fig. 4B–E). These results showed that inhibition of DYRK1A by UA may stabilize tubulin assembly through reducing tau phosphorylation. Meanwhile, the cell-free assay also provided evidence showing that UA is indeed a direct inhibitor of DYRK1A.

3.4. UA reversed Aβ-induced cell toxicity through regulating the inflammatory response

Previous evidence demonstrated that accumulation of Aβ exerts neurotoxicity and leads to cell death [14], and the cytotoxic effect of Aβ might be tau-dependent [15]. In our study, treatment with oligomeric Aβ (oAβ) caused BV-2 microglial cell death in a dose-dependently manner, with IC_{50} = 0.83 μM after exposure to oAβ for 24 h (Fig. 5A). We further showed that this cytotoxic effect was enhanced in DYRK1A/Tau-overexpressing cells, with IC_{50} = 0.11 μM after exposure to oAβ for 24 h (Fig. 5B). The addition of UA dose-dependently reversed the cell death which caused by oAβ, with IC_{50} = 0.33 μM (Fig. 5C). Moreover, UA alone had no impact on the viability of BV-2 cells (Fig. 5D). To reveal how UA provided a neuroprotective effect, the levels of inflammatory cytokines were

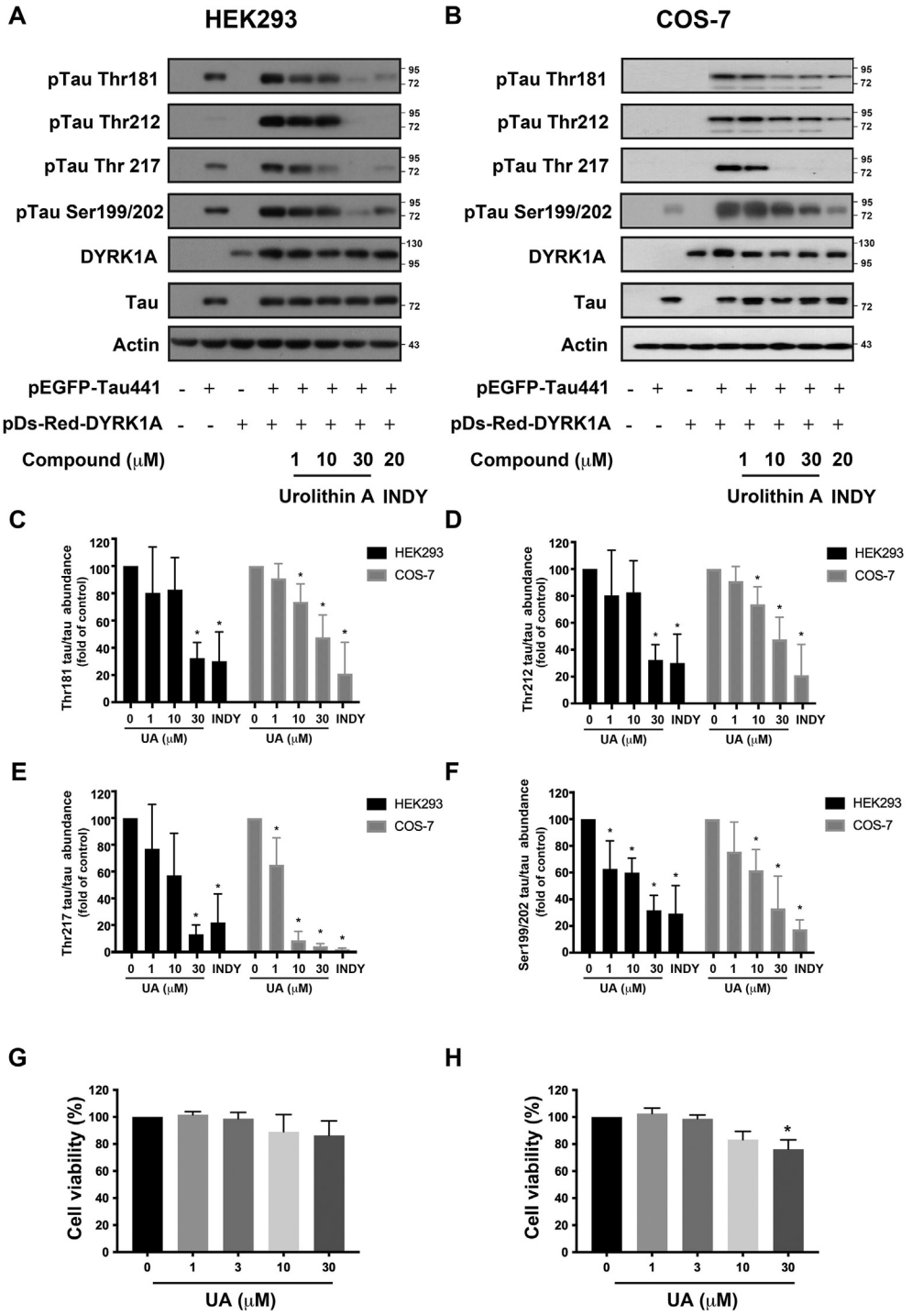

Fig. 3. ***Urolithin A (UA) inhibited tau phosphorylation in DYRK1A/Tau-overexpressed cells.*** *(A) HEK293 and (B) COS-7 cells were co-transfected with tau and DYRK1A and then treated with the indicated doses of UA and INDY for 24 h. Quantitative results are shown in C ~ F. The effect of UA on cell viability was assessed in (G) HEK293 and (H) COS-7 cells. Image J software was used to quantify band intensities. Data are presented as the mean (n = 3). *, p < 0.05 compared to the control group.*

examined, and results showed that oAβ significantly increased interleukin-6 (IL-6) and tumor necrosis factor-α (TNF-α) expressions and pretreatment with UA successfully reversed expressions of these inflammatory cytokines (Fig. 5E and F).

3.5. UA ameliorated spatial and learning memory impairment in vivo

To determine whether UA could be further used in the clinic, mice with memory deficits were used to

evaluate the effects of UA. OA is an inhibitor of protein phosphatase 1 (PP1) and phosphatase 2a (PP2A), and inhibition of PP1 or PP2A causes phosphorylation of the tau protein and fosters the further development of AD-like pathologies [16]. Fig. 6A shows the experimental procedure and treatment schedule. After habituation, mice were pretreated with vehicle or UA (100 mg/kg, intraperitoneally, daily) for three days, and then the vehicle or OA (100 ng/μL, intracerebroventricularly) was injected into the amygdala on the right side of the brain (Day 0). A Morris water maze was used to evaluate the cognitive functions on Day 16. Results showed that the latency to first entry to platform zone was significantly longer in OA-treated mice compared to the control group. The distance to reached the platform was also higher in OA-treated mice. On the other hand, mice pretreated with UA exhibited markedly reduced times and distances spent on finding the platform (Fig. 6B). Moreover, mice treated with OA failed to show preference for the correct quadrant, and pretreated with UA

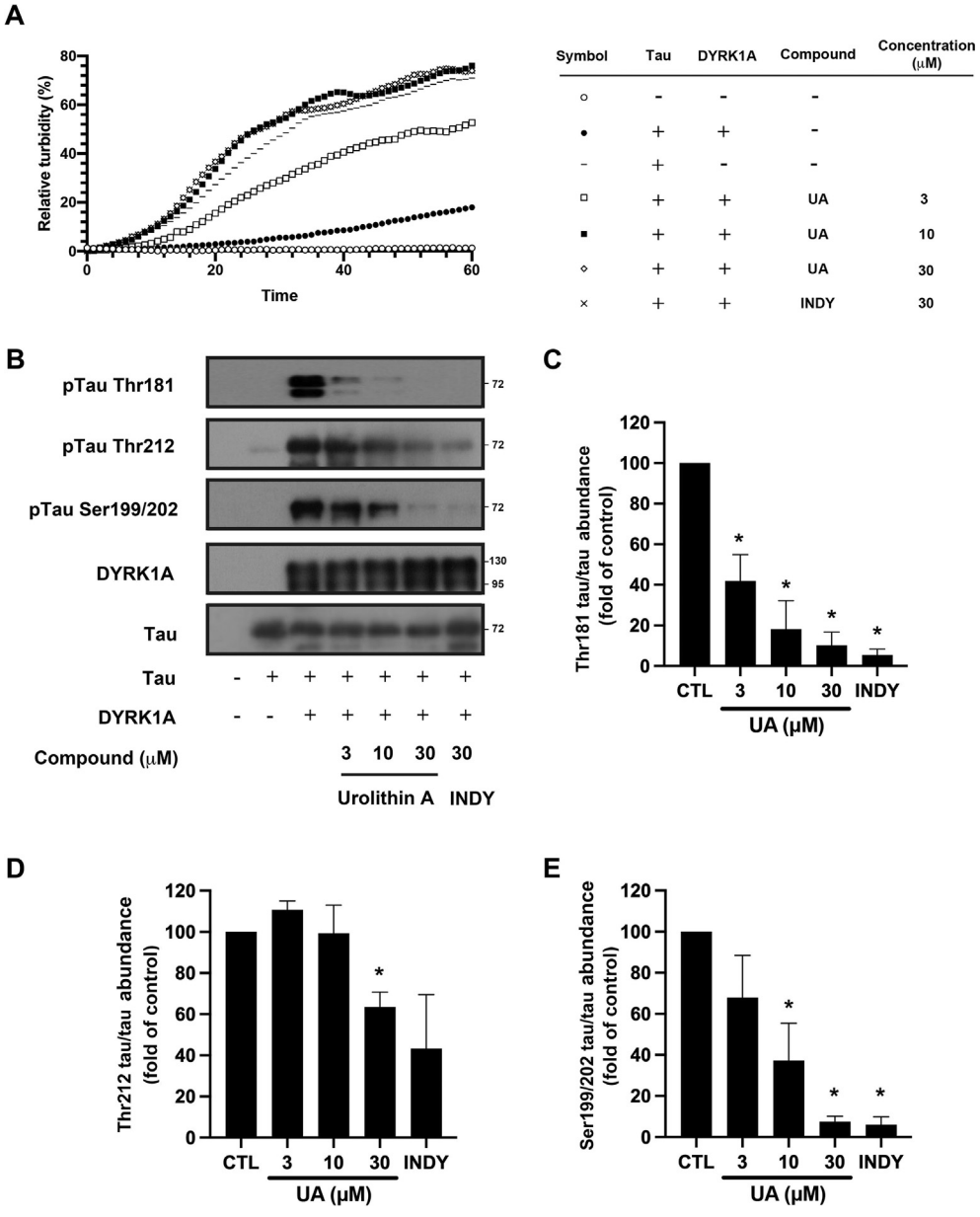

Fig. 4. ***Urolithin A (UA) stabilized tubulin polymerization by reducing tau phosphorylation in a cell-free system.*** *(A) The tau protein alone showed a steady increased in turbidity over time (–). Tau and DYRK1A together markedly reduced the turbidity (●). Co-treatment with UA dose-dependently rescued the effects of DYRK1A treatment. (B) UA dose-dependently decreased tau phosphorylation. Quantitative results are shown in C ~ E. Image J was used to quantify band intensities. Data are presented as the mean (n = 3). *, p < 0.05 compared to the control group.*

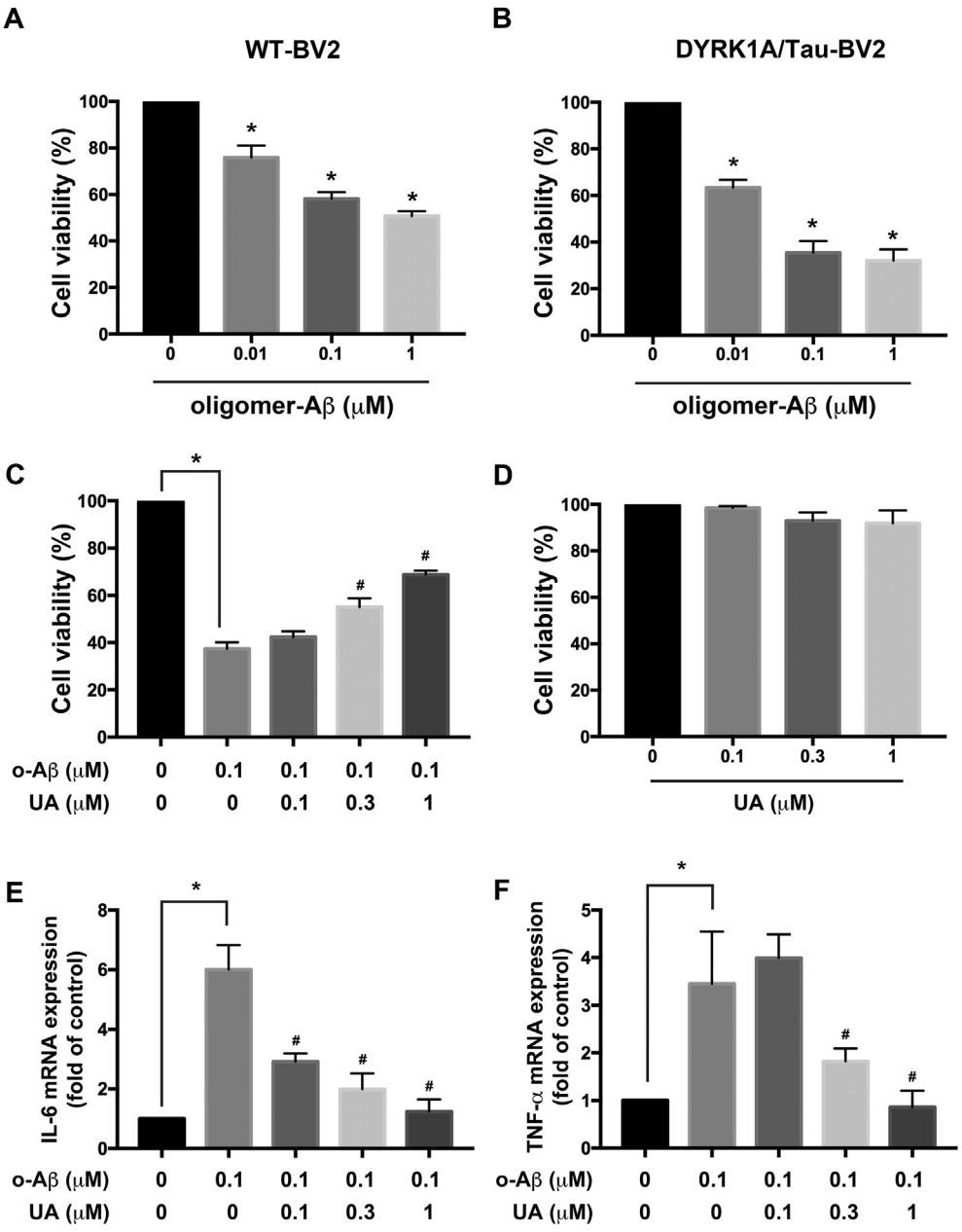

Fig. 5. ***Pretreatment with urolithin A (UA) reduced oligomeric β amyloid (oAβ)-induced inflammation and cell death.*** *(A) oAβ dose-dependently induced cell death in BV-2 cells. (B) BV-2 cells overexpressing DYRK1A enhanced oAβ-induced cell death. (C) Pretreatment with UA reversed oAβ-induced cell death in DYRK1A/Tau-BV2 cells. (D) UA alone had no effect on BV-2 cell viability. oAβ caused (E) interleukin-6 (IL-6) and (F) tumor necrosis factor-α (TNF-α) mRNA expressions, and these effects were reversed by UA. Data are presented as the mean (n = 3). *, p < 0.05 compared to the control group. #, p < 0.05 compared to the oAβ-treated group.*

reversed this result (Fig. 6C). A significant increase in the escape latency was found on Day 16 (test day) in OA group and treatment with UA decrease the time to find the correct platform (Fig. 6D). These results indicated that OA impaired the learning and memory abilities of mice, while treatment with UA reversed this memory defect. Body weight was measured every three days, and results showed that OA had caused slightly body weight loss on Day 3 which had soon recovered by Day 6. Mice treated with UA showed a steady increase in body weight (Fig. 6E). We further extracted protein from the hippocampus region of the mouse brain, it showed that OA increased the phosphorylation levels of Tau at Thr-212. In contrast, UA reversed this phenomenon (Fig. 6F).

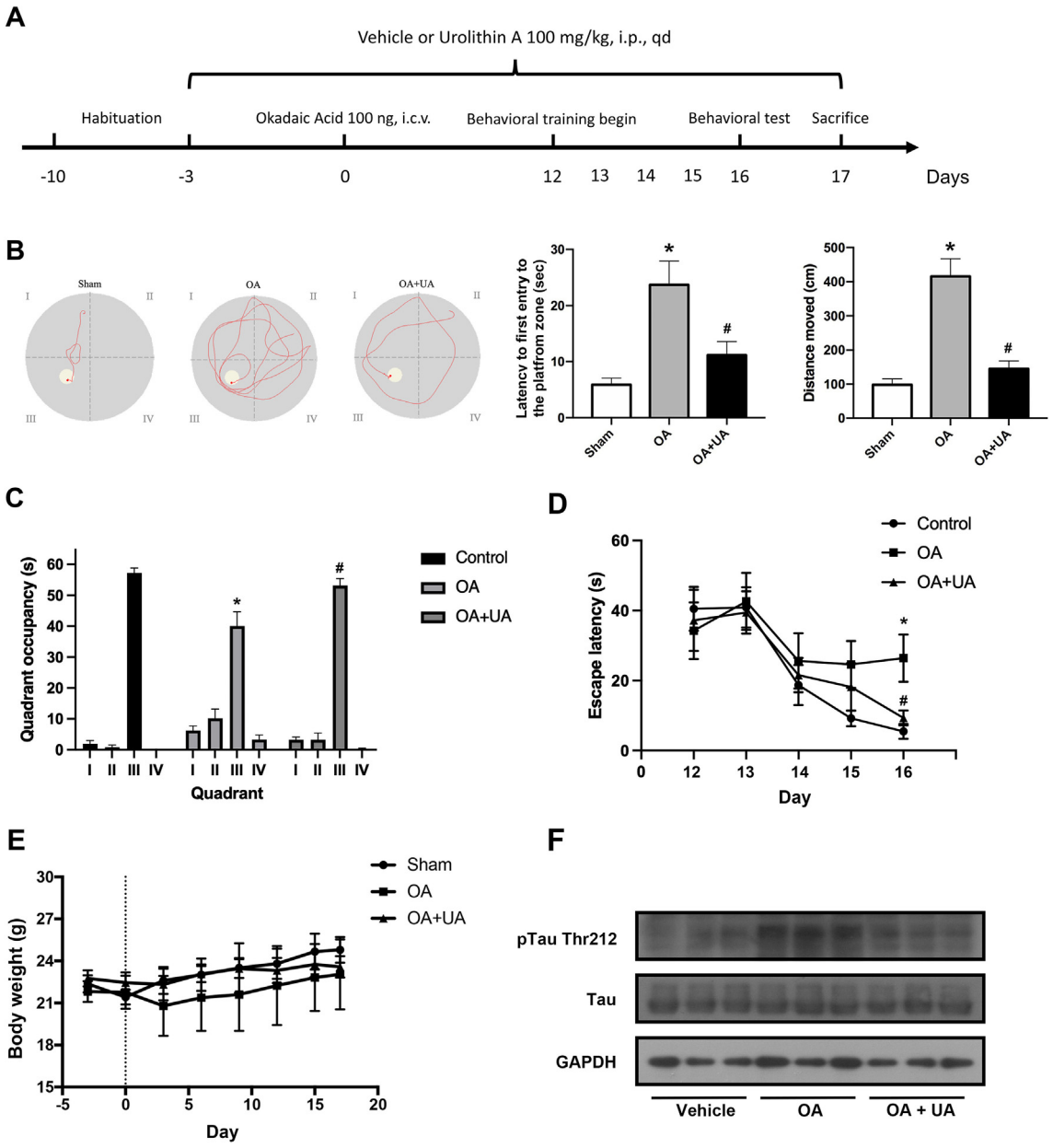

Fig. 6. ***Urolithin A (UA) improved AD-like pathology in an okadaic acid (OA)-induced animal model.*** *(A) Schematic overview of the experimental design for the AD mouse models. Results of Morris water maze was measured by (B) Latency of first entry time to the platform zone and total distance moved. (C) Percentage of time spent in each quadrant. (D) Latencies to reach platform. (E) Body weight was measured every 3 days after an intracerebroventricular injection of OA. (n = 8 in each group). (F) Expressions levels of phosphorylated Tau at Thr212 in different groups. *, p < 0.05 compared to the sham group. #, p < 0.05 compared to the OA-treated group.*

4. Discussion and conclusion

UA is a product of ellagitannin metabolized by intestinal microorganisms [17]. The benefits of UA to human health include anticancer, anti-inflammatory, and anti-aging effects [7]. According to previous research, UA can cross the blood–brain barrier (BBB) and be absorbed by the brain [5], which means that UA may be able to be used for neurodegenerative diseases. In an APP/PS1 AD mouse model, UA reduced the level of Aβ in the cerebral cortex and hippocampus, and effectively prevented neuronal cell death. Moreover, UA inhibited the production of inflammatory signals in APP/PS1 mice by reducing activities of microglia and astrocytes [8].

Compared to a previous study, which mainly focused on studying the effect of UA on Aβ, our work revealed that UA is also involved in pathologic

tau formation through regulating DYRK1A activity [8]. UA forms hydrophobic interactions with side chains of residues V173, A186, L241, L294 and V306 to allow it to anchor to the DYRK1A active site. DYRK1A is an interesting kinase which is involved in tau protein phosphorylation and has garnered considerable attention due to its role in neurodegenerative diseases such as AD and Down syndrome [18,19]. In AD patients, the levels of DYRK1A are higher than in healthy volunteers [19]. Overexpression of DYRK1A directly induces hyperphosphorylation of tau and is related to brain atrophy and cognitive decline [20]. In addition, DYRK1A also indirectly activates an alternative splicing factor (ASF) to regulate the alternative splicing of tau exon 10 [21]. Furthermore, DYRK1A overexpression enhanced the phosphorylation of presenilin 1 (PS1) at Thr354 [22], increasing the activity of γ-secretase and further leading to Aβ formation. Together, these data indicated that inhibiting the activity of DYRK1A may be a potential strategy for AD treatment.

Tau proteins are enriched in neuronal cells, which regulate tubulin stability. Tau binds to microtubules to support neurite differentiation and axon transportation [12]. Abnormal tau phosphorylation is an important feature in neurodegenerative diseases, especially AD. Phosphorylation at Thr212 significantly induced tau aggregation, which further induced the cell death in R406W CHO cells [23]. Phosphorylated tau at Ser396/404 is highly related to the aging brain and mitochondrion dysfunction [24]. Tau phosphorylation at Thr181 [25] and Thr217 [26] was proven to be a diagnostic biomarker of the early stage of AD. Previous report has shown that UA may induce mitophagy through activation of SIRT, AMPK and inhibition of mTOR [27]. Moreover, UA inhibits tau phosphorylation by stimulating mitophagy machinery [28]. In current study, we showed that UA successfully reversed tau phosphorylation which caused by DYRK1A overexpression at multiple sites including Ser199/202, Thr212, Thr181 and Thr217 (Fig. 3) and further stabilized tubulin polymerization (Fig. 4).

Neuroinflammation is also a prominent feature in the pathogenesis of AD, as many studies pointed out that the immune system is hyper-activated, and elevated levels of inflammatory cytokines were observed in AD [29]. TNF-α and IL-6 are two major cytokines which are induced by Aβ stimulation and further causes neuronal cell death [30]. Reducing the inflammatory response by anti-inflammatory agents showed promising neuroprotective effects in cell culture and animals, although the clinical benefits are still being debated [31]. In our study, we found that pretreatment with UA significantly reduced the inflammatory response which caused by oAβ; furthermore, UA also reversed oAβ-induced cell death. Previous studies have shown that UA was a potent anti-inflammatory agent which inhibited NF-κB, MAPK and PI3K/Akt/mTOR signaling in bone-marrow-derived macrophages challenged with LPS [32]. In a colitis rat model, UA also reduced the inflammatory response by reducing inducible iNOS, COX-2, PTGES and PGE_2 [33]. On the other hand, inhibition of DYRK1A decreased the levels of IL-6, IL-8, IL-1β and TNF-α which caused by LPS and showed potential to improve symptoms of osteoarthritis [34]. Together, these data indicated that UA reduced oAβ-induced cell death by inhibiting DYRK1A activity to decrease inflammatory response.

A previous study has used APP/PS1 transgenic mice to showed that UA provided neuroprotective effects against AD [8]; however, that animal model is more relevant to Aβ. In an attempt to study the effect of UA on tau pathology, a local injection of OA was used to mimic an AD tauopathic model. OA is a PP1 and PP2A inhibitor which causes tau phosphorylation and tangle formation without amyloid pathology [35]. Our study showed that pretreatment with UA ameliorated cognitive impairment in an OA-induced animal model. Since OA is also an inducer of IL-6 and TNF-α [36,37], part of the effects of UA may also come from its ability to reduce inflammatory responses.

In conclusion, our data demonstrated that UA is a potent DYRK1A inhibitor. In DYRK1A/Tau-overexpressing cells, administration of UA reduced tau phosphorylation at multiple sites and further stabilized tubulin polymerization. Furthermore, UA decreased the inflammatory response and reversed neuronal cell death which caused by oAβ. Finally, daily administration of UA improved memory in an AD-like animal model. Although several kinases have been implicated in the development of Alzheimer's disease, including CDK5 and GSK3β, targeting these kinases has shown limited success in clinical trials. This indicates that the pathogenesis of AD is more complex than previously anticipated. DYRK1A was found to regulate the activity of CDK5 in glioblastoma cells [38], while in another study, it was shown to phosphorylate GSK3β and control various signaling pathways in obesity [39]. Our findings, together with these studies, suggest that DYRK1A could be a promising therapeutic target for AD, given its potential to regulate multiple pathways involved in the disease's pathogenesis.

Author contributions

Huang-Ju Tu: Conceptualization, Visualization, Data curation, Validation, Manuscript writing.

Chih-Jou Su: Data curation, Visualization, Manuscript writing.

Chao-Shiang Peng: Data curation, Visualization.

Tony Eight Lin: Computational modeling analysis, Visualization.

Wei-Chun HuangFu: Conceptualization, Supervision, Validation.

Tsong-Long Hwang: Conceptualization, Funding acquisition, Supervision.

Shiow-Lin Pan: Conceptualization, Funding acquisition, Supervision, Validation.

Funding

This study was supported by the Ministry of Science and Technology, Taiwan (MOST 110-2320-B038-040-MY3) and Chang Gung Memorial Hospital, Taiwan (CMRPF1J0051-3).

Conflict of interest

The authors declare that they have no known competing financial interests or personal relationships that could have appeared to influence the work reported in this paper.

Acknowledgements

We appreciate Dr. Yun-Ru Chen from Academia sinica for providing BV-2 cell line. We also thank Dr. Chiung-Yuan Ko from Taipei Medical University for giving human tau 441 plasmid.

References

[1] Cummings J, Lee G, Zhong K, Fonseca J, Taghva K. Alzheimer's disease drug development pipeline: 2021. Alzheimers Dement (N Y) 2021;7:e12179.
[2] Masters CL, Bateman R, Blennow K, Rowe CC, Sperling RA, Cummings JL. Alzheimer's disease. Nat Rev Dis Primers 2015;1:15056.
[3] Lombardi G, Crescioli G, Cavedo E, Lucenteforte E, Casazza G, Bellatorre AG, et al. Structural magnetic resonance imaging for the early diagnosis of dementia due to Alzheimer's disease in people with mild cognitive impairment. Cochrane Database Syst Rev 2020;3:CD009628.
[4] Fu LM, Li JT. A systematic review of single Chinese herbs for Alzheimer's disease treatment. Evid Based Complement Alternat Med 2011;2011:640284.
[5] Yuan T, Ma H, Liu W, Niesen DB, Shah N, Crews R, et al. Pomegranate's neuroprotective effects against Alzheimer's disease are mediated by urolithins, its ellagitannin-gut microbial derived metabolites. ACS Chem Neurosci 2016;7:26−33.
[6] Tomas-Barberan FA, Garcia-Villalba R, Gonzalez-Sarrias A, Selma MV, Espin JC. Ellagic acid metabolism by human gut microbiota: consistent observation of three urolithin phenotypes in intervention trials, independent of food source, age, and health status. J Agric Food Chem 2014;62:6535−8.
[7] D'Amico D, Andreux PA, Valdes P, Singh A, Rinsch C, Auwerx J. Impact of the natural compound urolithin A on health, disease, and aging. Trends Mol Med 2021;27:687−99.
[8] Gong Z, Huang J, Xu B, Ou Z, Zhang L, Lin X, et al. Urolithin A attenuates memory impairment and neuroinflammation in APP/PS1 mice. J Neuroinflammation 2019;16:62.
[9] Lee HJ, Jung YH, Choi GE, Kim JS, Chae CW, Lim JR, et al. Urolithin A suppresses high glucose-induced neuronal amyloidogenesis by modulating TGM2-dependent ER-mitochondria contacts and calcium homeostasis. Cell Death Differ 2021;28:184−202.
[10] Burley SK, Bhikadiya C, Bi C, Bittrich S, Chen L, Crichlow GV, et al. RCSB Protein Data Bank: powerful new tools for exploring 3D structures of biological macromolecules for basic and applied research and education in fundamental biology, biomedicine, biotechnology, bioengineering and energy sciences. Nucleic Acids Res 2021;49:D437−51.
[11] Friesner RA, Banks JL, Murphy RB, Halgren TA, Klicic JJ, Mainz DT, et al. Glide: a new approach for rapid, accurate docking and scoring. 1. Method and assessment of docking accuracy. J Med Chem 2004;47:1739−49.
[12] Alonso AD, Cohen LS, Corbo C, Morozova V, ElIdrissi A, Phillips G, et al. Hyperphosphorylation of tau associates with changes in its function beyond microtubule stability. Front Cell Neurosci 2018;12:338.
[13] Barbier P, Zejneli O, Martinho M, Lasorsa A, Belle V, Smet-Nocca C, et al. Role of tau as a microtubule-associated protein: structural and functional aspects. Front Aging Neurosci 2019;11:204.
[14] Kadowaki H, Nishitoh H, Urano F, Sadamitsu C, Matsuzawa A, Takeda K, et al. Amyloid beta induces neuronal cell death through ROS-mediated ASK1 activation. Cell Death Differ 2005;12:19−24.
[15] Bloom GS. Amyloid-beta and tau: the trigger and bullet in Alzheimer disease pathogenesis. JAMA Neurol 2014;71:505−8.
[16] Kamat PK, Rai S, Swarnkar S, Shukla R, Nath C. Molecular and cellular mechanism of okadaic acid (OKA)-induced neurotoxicity: a novel tool for Alzheimer's disease therapeutic application. Mol Neurobiol 2014;50:852−65.
[17] Espín JC, Larrosa M, García-Conesa MT, Tomás-Barberán F. Biological significance of urolithins, the gut microbial ellagic acid-derived metabolites: the evidence so far. Evid Based Complement Alternat Med 2013;2013:270418.
[18] Kimura R, Kamino K, Yamamoto M, Nuripa A, Kida T, Kazui H, et al. The DYRK1A gene, encoded in chromosome 21 Down syndrome critical region, bridges between beta-amyloid production and tau phosphorylation in Alzheimer disease. Hum Mol Genet 2007;16:15−23.
[19] Ferrer I, Barrachina M, Puig B, Martinez de Lagran M, Marti E, Avila J, et al. Constitutive Dyrk1A is abnormally expressed in Alzheimer disease, Down syndrome, Pick disease, and related transgenic models. Neurobiol Dis 2005;20:392−400.
[20] Ryoo S-R, Jeong HK, Radnaabazar C, Yoo J-J, Cho H-J, Lee H-W, et al. DYRK1A-mediated hyperphosphorylation of tau. J Biol Chem 2007;282:34850−7.
[21] Shi J, Zhang T, Zhou C, Chohan MO, Gu X, Wegiel J, et al. Increased dosage of Dyrk1A alters alternative splicing factor (ASF)-regulated alternative splicing of tau in Down syndrome. J Biol Chem 2008;283:28660−9.
[22] Ryu YS, Park SY, Jung MS, Yoon SH, Kwen MY, Lee SY, et al. Dyrk1A-mediated phosphorylation of Presenilin 1: a functional link between Down syndrome and Alzheimer's disease. J Neurochem 2010;115:574−84.
[23] Alonso AD, Di Clerico J, Li B, Corbo CP, Alaniz ME, Grundke-Iqbal I, et al. Phosphorylation of tau at Thr212, Thr231, and Ser262 combined causes neurodegeneration. J Biol Chem 2010;285:30851−60.

[24] Torres AK, Jara C, Olesen MA, Tapia-Rojas C. Pathologically phosphorylated tau at S396/404 (PHF-1) is accumulated inside of hippocampal synaptic mitochondria of aged Wild-type mice. Sci Rep 2021;11:4448.
[25] Karikari TK, Pascoal TA, Ashton NJ, Janelidze S, Benedet AL, Rodriguez JL, et al. Blood phosphorylated tau 181 as a biomarker for Alzheimer's disease: a diagnostic performance and prediction modelling study using data from four prospective cohorts. Lancet Neurol 2020;19:422−33.
[26] Janelidze S, Stomrud E, Smith R, Palmqvist S, Mattsson N, Airey DC, et al. Cerebrospinal fluid p-tau217 performs better than p-tau181 as a biomarker of Alzheimer's disease. Nat Commun 2020;11:1683.
[27] Jayatunga DPW, Hone E, Khaira H, Lunelli T, Singh H, Guillemin GJ, et al. Therapeutic potential of mitophagy-inducing microflora metabolite, urolithin A for Alzheimer's disease. Nutrients 2021;13.
[28] Fang EF, Hou Y, Palikaras K, Adriaanse BA, Kerr JS, Yang B, et al. Mitophagy inhibits amyloid-beta and tau pathology and reverses cognitive deficits in models of Alzheimer's disease. Nat Neurosci 2019;22:401−12.
[29] Kinney JW, Bemiller SM, Murtishaw AS, Leisgang AM, Salazar AM, Lamb BT. Inflammation as a central mechanism in Alzheimer's disease. Alzheimers Dement (N Y) 2018;4:575−90.
[30] Wood LB, Winslow AR, Proctor EA, McGuone D, Mordes DA, Frosch MP, et al. Identification of neurotoxic cytokines by profiling Alzheimer's disease tissues and neuron culture viability screening. Sci Rep 2015;5:16622.
[31] Walker D, Lue LF. Anti-inflammatory and immune therapy for Alzheimer's disease: current status and future directions. Curr Neuropharmacol 2007;5:232−43.
[32] Abdelazeem KNM, Kalo MZ, Beer-Hammer S, Lang F. The gut microbiota metabolite urolithin A inhibits NF-kappaB activation in LPS stimulated BMDMs. Sci Rep 2021;11:7117.
[33] Larrosa M, Gonzalez-Sarrias A, Yanez-Gascon MJ, Selma MV, Azorin-Ortuno M, Toti S, et al. Anti-inflammatory properties of a pomegranate extract and its metabolite urolithin-A in a colitis rat model and the effect of colon inflammation on phenolic metabolism. J Nutr Biochem 2010;21:717−25.
[34] Deshmukh V, O'Green AL, Bossard C, Seo T, Lamangan L, Ibanez M, et al. Modulation of the Wnt pathway through inhibition of CLK2 and DYRK1A by lorecivivint as a novel, potentially disease-modifying approach for knee osteoarthritis treatment. Osteoarthritis Cartilage 2019;27:1347−60.
[35] Baker S, Gotz J. A local insult of okadaic acid in wild-type mice induces tau phosphorylation and protein aggregation in anatomically distinct brain regions. Acta Neuropathol Commun 2016;4:32.
[36] Tebo JM, Hamilton TA. Okadaic acid stimulates inflammatory cytokine gene transcription in murine peritoneal macrophages. Cell Immunol 1994;153:479−91.
[37] Suuronen T, Huuskonen J, Nuutinen T, Salminen A. Characterization of the pro-inflammatory signaling induced by protein acetylation in microglia. Neurochem Int 2006;49:610−8.
[38] Chen B, McCuaig-Walton D, Tan S, Montgomery AP, Day BW, Kassiou M, et al. DYRK1A negatively regulates CDK5-SOX2 pathway and self-renewal of glioblastoma stem cells. Int J Mol Sci 2021:22.
[39] Song WJ, Song EA, Jung MS, Choi SH, Baik HH, Jin BK, et al. Phosphorylation and inactivation of glycogen synthase kinase 3beta (GSK3beta) by dual-specificity tyrosine phosphorylation-regulated kinase 1A (Dyrk1A). J Biol Chem 2015;290:2321−33.